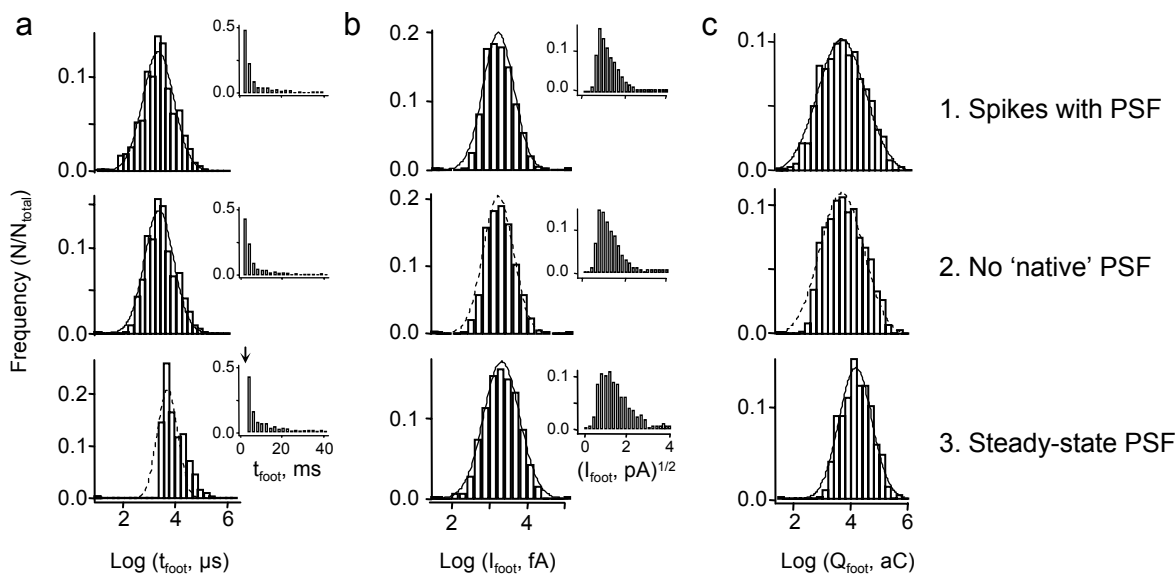


Supplementary Figure 1. Finding spike beginning (T_{bkg1}) and end (T_{bkg2}).

Dashed lines represent spike baseline and percentages of I_{max} on current traces or zero line of the differential traces. Circles on dI/dt trace indicate interceptions with zero. The scale-bars are 20 pA, 20 pA/ms and 5 ms. Upper sub-panels show amperometric current, lower sub-panels - its time derivative, except **d**. **(a)** Analysis of spikes on traces with stable background current. T_{max} and $T(dI/dt)_{max}$ are times at the maxima of the current and dI/dt , correspondingly. **(b)** Example of fitting the current from 25% of I_{max} on spike rising phase to T_{bkg2} with exponentially modified Gaussian curve. Note that the maximum of the fit curve is lower than the maximum of current; this discrepancy might be bigger for smaller spikes or on recordings with higher noise. **(c and d)** Searching for steady state that precedes a spike or the one on PSF. The same spike at different scales is shown on **c** and **d**. Vertical lines on **d** show trace segments with duration ΔT_{min} (upper) and $2^* \Delta T_{min}$ (lower); horizontal solid lines represent average current within each segment; arrowheads indicate steady states found by the routine. To find the steady state before the spike, ΔT_{min} is set to spike width at $T(dI/dt)_{max}$ (duration between points 1 and 1' on **a**). To find PSF steady state, ΔT_{min} is set to half of the user-defined minimal foot duration. **(e)** The presence of high-frequency noise (arrowhead) affects the accuracy of T_{bkg2} determination, leading to underestimation of amperometric charge and a misrepresentation of falling phase fit constants. **(f)** Analysis of spikes with uneven baseline. Horizontal dotted line represents background current preceding the first spike. See **Supplementary Methods** online for more details.



Supplementary Figure 2. Statistical analysis of different foot subpopulations

Only non-overlapping spikes with $I_{\max} > 3$ pA, and only PSF with amplitude $> 2 \cdot SD_1$ were analyzed (1011 amperometric spikes). The **figure** shows histograms of foot duration (a) amplitude (b) and charge (c) from three PSF subpopulations: (1) all detected feet, (2) feet with durations longer than predicted for 'native' PSF and (3) feet with steady states longer than 2 ms. 'Native' feet are predicted by mathematical simulations of instantaneous transmitter release¹³ and calculated as $0.33 \times t_{\text{rise}}$ (50-90%). The units were chosen so that all parameter values are larger than one, thus yielding positive Log values. The histograms of Log-transformed values were fit by Gaussian curves; superimposed lines represent fits of the data that either did not deviate (data are normally distributed, solid lines), or did deviate (dotted lines) from the Gaussian fit by 'runs' test. The insets on (a) show histograms of non-transformed t_{foot} values, which follow single-exponential distribution, in agreement with previously published data¹⁸. Note that the first bin has zero datapoints on the histogram of steady-state PSF durations (arrow). The insets on (b) show square root transformed I_{foot} values. For the **table**, the median values of amperometric spike and PSF parameters from 24 cells were calculated for each cell; data are presented as mean \pm SD of parameter values between the cells.

	Spike					PSF			
	I_{\max} [pA]	$t_{1/2}$ [ms]	Q § [molecules]	t_{rise} §§ [ms]	Rise [pA/ms]	I_{foot} [pA]	t_{foot} [ms]	Q_{foot} § [molecules]	% of events&
All spikes	25.7 \pm 14.4	4.7 \pm 1.8	560,000 \pm 230,000	0.74 \pm 0.21	19.1 \pm 12.1				100 %
Spikes with PSF	34.6 \pm 17.3*	4.3 \pm 1.6	710,000 \pm 320,000*	0.69 \pm 0.20	27.1 \pm 17.4*	1.8 \pm 0.9	3.2 \pm 3.7	24,000 \pm 19,000	82 %
No 'native' PSF #	38.1 \pm 17.7*	4.2 \pm 1.6	760,000 \pm 350,000*	0.68 \pm 0.20	30.9 \pm 17.6*	2.0 \pm 0.9	3.5 \pm 3.9	29,000 \pm 24,000	75 %
Steady-state PSF	with	42.0 \pm 18.1*	920,000 \pm 370,000*	0.74 \pm 0.58	32.5 \pm 20.4*	2.1 \pm 0.8	6.7 \pm 4.6**	57,000 \pm 39,000**	45 %
	without	15.4 \pm 8.1**	5.2 \pm 2.4	380,000 \pm 140,000**	0.80 \pm 0.28	12.6 \pm 9.0**			55 %

§ - The number of released catecholamine molecules was calculated from amperometric charge as described in Fig. 3 legend

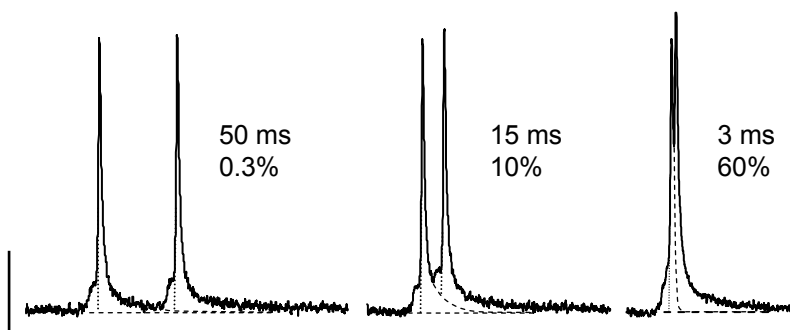
§§ - Risettime between 25% and 75% of I_{\max} excluding the foot

& - Fraction of all spikes

- PSF with durations $> 0.246 \cdot t_{\text{rise}}$

* - Significantly different from 'All spikes' group with $p < 0.05$ by Mann-Whitney rank sum test

** - Significantly different from all other groups with $p < 0.05$ by Mann-Whitney rank sum test



Supplementary Figure 3. Analysis of overlapping spikes

Any two amperometric spikes are considered overlapping if (i) the current at the end of the first spike is higher than at its beginning (uneven baseline), and (ii) the duration between the end of the first spike and beginning of the next is less than the average (among all spikes) $t_{1/2}$. The program first finds all amperometric spikes (see **Supplementary Methods**) and then checks for the overlaps. The baseline of the second overlapping spike is approximated using exponential fit constants of the falling phase of the first spike; if the fit is double-exponential, the slower τ is used. **Figure**. Overlaps of various degrees were generated by summing two identical recordings one of which was offset by a certain duration; the first and second spikes are therefore identical. Numbers next to the spikes indicate the offset and the extent of overlap. The latter was calculated as $I_{saddle}/I_{max} * 100$, where I_{saddle} is the current at the minimum between the spikes and I_{max} is the amplitude of the first spike. Dashed lines represent spike baselines; dotted lines show PSF. Scale-bars are 50 pA and 50 ms. Data in the **Table** show % changes of the values for spike characteristics measured from overlapping spikes compared to those measured on the original singlet spike. Parameters that deviate from the true values by more than 15% are highlighted. Note that the differences between the original and the overlapping spike characteristics will be different when real spikes with unequal shapes are analyzed. Missing values for τ_2 indicate that spike's falling phase was fit with single exponential function.

Overlap	Spike	$t_{1/2}$ [ms]	I_{max} [pA]	Q [molecules]	t_{rise} [ms]	Rise [pA/ms]	Fall, τ_1 [ms]	Fall, τ_2 [ms]	I_{foot} [pA]	t_{foot} [ms]	Q_{foot} [molecules]
0.3 %	1	98	99	93	98	101	104	110	101	95	95
	2	100	100	107	98	103	98	104	112	90	101
5 %	1	99	99	87	101	98	80	91	96	92	89
	2	100	100	113	100	101	98	101	81	63	42
10 %	1	100	99	93	101	97	102	81	112	75	84
	2	97	97	107	99	97	98	112	65	66	47
25 %	1	107	106	85	101	106	99		125	73	93
	2	103	104	115	107	98	117	155	61	9	8
40 %	1	110	109	85	114	96	99		125	92	116
	2	100	105	115	115	94	121	166	66	4	4
60 %	1	117	109	77	109	102	76		144	90	131
	2	102	107	123	133	87	123	170	42	1	1

Supplementary Table. Statistical analysis of different spike subpopulations

Comparison of amperometric events (i) the falling phase of which was better fit with single- or double-exponential functions, and (ii) the t_{rise} of which was higher or lower than the cutoff. The falling phase of each spike between 75% of I_{max} and T_{bkg2} was fit with single- and double-exponential functions and the latter was employed if $\chi^2(\text{single}) / \chi^2(\text{double})$ was more than two. Of 1011 spikes, 458 (45%) were better fit with double exponentials. The cutoff for t_{rise} was set to 1.5 ms - more than 3*SD higher than the population's mean. Of 1011 spikes, 156 (15 %) had t_{rise} longer than the cutoff. Only non-overlapping spikes with $I_{max} > 3$ pA and only PSF with $I_{foot} > 2*SD_1$ were analyzed. The median of each parameter value was calculated from 24 cells; data are presented as mean \pm SD of parameter values between the cells.

	I_{max} [pA]	$t_{1/2}$ [ms]	Q^{\S} [molecules]	$t_{rise}^{\S\S}$ [ms]	Rise slope [pA/ms]	Fall, τ_1 [ms]	Fall, τ_2 [ms]	spikes with PSF	with steady- state PSF [#]
All spikes	25.7 \pm 14.4	4.7 \pm 1.8	560,000 \pm 230,000	0.74 \pm 0.21	19.1 \pm 12.1	4.1 \pm 2.6	10.4 \pm 4.2	82 %	45 %
Single exp	9.2 \pm 2.4	6.7 \pm 2.0	290,000 \pm 80,000	0.99 \pm 0.31	4.9 \pm 1.7	7.4 \pm 2.5	-	69 %	30 %
Double exp	67.7 \pm 27.5*	3.2 \pm 1.0*	1,190,000 \pm 520,000*	0.58 \pm 0.14*	62.0 \pm 33.2*	1.9 \pm 0.6*	10.4 \pm 4.2**	96 %	57 %
$t_{rise} > 1.5$ ms	7.3 \pm 2.9	11.2 \pm 2.8	400,000 \pm 240,000	2.32 \pm 0.41	1.8 \pm 0.9	11.1 \pm 3.9 ^{&}	24.8 \pm 14.4	58 %	32 %
$t_{rise} < 1.5$ ms	31.3 \pm 15.8*	4.1 \pm 1.4*	650,000 \pm 330,000*	0.65 \pm 0.12*	25.8 \pm 14.9*	3.5 \pm 2.1*	10.1 \pm 4.0*	87 %	45 %

[§] - The number of released catecholamine molecules was calculated from amperometric charge as described in Fig. 3 legend

^{§§} - Duration between 25% and 75% of I_{max} excluding the foot

[#] - Fraction of spikes that displayed PSF with steady-states longer than 2 ms

[&] - Includes both single- and double-exp τ_1

* - Significantly different from single-exp or $t_{rise} > 1.5$ ms with $p < 0.05$ by Mann-Whitney rank sum test

** - Significantly different from τ_1 of both single- and double-exp with $p < 0.05$ by Mann-Whitney rank sum test

Analysis of Exocytotic Events Recorded by Amperometry

Eugene V. Mosharov & David Sulzer

Supplementary Methods

Digital filters

Gaussian filters are similar to Bessel filters (albeit much easier to program) in that they both have constant group delay and do not produce ripples in the time domain^{1,2}. We employ two types of digital low-pass Gaussian filters, a genuine infinite impulse response (IIR) Gaussian filter and a finite impulse response (FIR) binomial smoothing. For Gaussian IIR filter, the fast Fourier transform of an amperometric trace is multiplied by a Gaussian of selected width to achieve -3dB attenuation of frequency at a desired cutoff (F_c , Hz). The advantage of this filter is that its corner frequency can be adjusted precisely in a wide range of values. The Gaussian is computed as:

$$G(x) = \exp\left(-\frac{x^2}{\sigma^2}\right); \text{ where } \sigma = \frac{Ampl_{cutoff}}{\sqrt{-\ln(F_c)}} \text{ and } Ampl_{cutoff} = \frac{1}{\sqrt{2}}$$

Binomial FIR filter convolves the data with normalized coefficients derived from Pascal's triangle at a level equal to the smoothing parameter³. Since this filter does not employ a Fourier transforms of the data, it requires much less computation time and is easier to use with large data files, such as neuronal amperometric traces that are recorded at a high sampling rate and may consist of millions of data-points. As a FIR filter, binomial smoothing has a more stable frequency response than an IIR Binomial filter. The following empirical formula can be used to express the level of binomial smoothing from Igor Pro (*Coeff*, the half-width of the base of Pascal's triangle) in the units of cutoff frequency:

$$F_c[\text{Hz}] = A \times SR \times \text{Coeff}^B, \text{ where } A = 0.1809, B = -0.4815 \text{ and } SR \text{ is sampling rate in Hz.}$$

As seen from the formula, the dependence between the binomial coefficients and desired F_c is a power function. This and the fact that *Coeff* is an integer create the major drawbacks of this filter: it has an F_c limit (Binomial 1 smoothing), and its steps can become too wide at higher frequencies making it difficult to accurately adjust the cutoff.

The choice of an 'optimal' filter for a particular type of recording is a complicated issue². The two-step filtering protocol shown in **Box 1** of the manuscript, however, simplifies the task by allowing to choose one filter (F_{c1} -3dB cutoff frequency higher than the signal frequency) that does not distort spike shapes and another one (lower F_{c2}) that increases signal-to-noise ratio sufficiently for events detection. The initial estimate for an appropriate filter cutoffs can be made from the maximum of the first derivative of amperometric current⁴, which corresponds to a spike with the fastest rising slope. The ratio of dl/dt amplitude to the amplitude of the corresponding spike on the non-differentiated trace (the latter is roughly estimated as delta current between two time-points at the intercepts of dl/dt with zero to the left and to the right of dl/dt maximum) represents twice the frequency of this 'fastest' spike ($F_{sp(max)}$). Next, $2 * F_{sp(max)}$ and $0.5 * F_{sp(max)}$ can be used as the initial F_{c1} and F_{c2} , correspondingly. In practice, because of the presence of very high frequency noise, $F_{sp(max)}$ values found on an unfiltered amperometric trace are often overestimated for relatively slow spikes found on LDCV recordings. To counter this, the routine incorporated in our program filters the recording with $3 * F_{sp(max)}$ Gaussian filter, which approximately equals the cutoff of a filter that will not affect the amplitude of the spike with a width $= 1 / F_{sp(max)}^2$, and then repeats the procedure for finding the $F_{sp(max)}$ described above. Finally, if the differentiated trace is used for spike detection, the differential is filtered at $F_{c3} = F_{sp(max)}$, as dl/dt frequency is approximately two fold higher than that of the non-differentiated trace.

Although this procedure helps to choose initial values for the filters cutoffs, further adjustments are usually required, including visual examination of a trace generated by subtracting the recording before and after the filtering - appearance of profound maxima on this trace indicates reduction of signal amplitude. It should be emphasized that all amperometric traces in an experimental series have to be filtered using the same set of filters. Therefore, the choice of the filters should be made prior to analysis using representative recordings from all experimental groups and the filter with the highest cutoff frequency should be used for all traces. Empirical values for LDCV and SSV recordings are as follows. For amperometric recordings from rat chromaffin cell (sampling frequency 10-25 kHz): $F_{sp(max)} = 200-1000$ Hz, $F_{c1} = 500-1000$ Hz, $F_{c2} = 100-400$ Hz, $F_{c3} = 200-1000$ Hz. For recordings from dopamine midbrain neurons: (sampling frequency 100-200 kHz): $F_{sp(max)} = 5-10$ kHz, $F_{c1} = 10-20$ kHz, $F_{c2} =$ not used, $F_{c3} = 5-10$ kHz.

Algorithms for finding spike baseline

The first parameter determined for a spike, the location of its maximum T_{max} , can be reliably evaluated by a protocol described by Borges's laboratory where it is found between $T(dI/dt)_{max}$ and the time point having the same current value on the descending segment of the spike⁵ (**Supplementary Fig. 1a**, points 1 and 1'). To improve the accuracy of T_{max} approximation on spikes with low signal-to-noise ratio, later in the analysis the whole spike or its topmost segment can be fit with exponentially modified Gaussian curve⁶ (**Supplementary Fig. 1b**).

If spikes are detected using SD_1 and the background current is stable with an average value I_{bkg} , the algorithms for finding spike beginning (T_{bkg1}), and end (T_{bkg2}) are straightforward - these are the first time-points to the left and to the right of T_{max} at the I_{bkg} current level⁷. Similarly, if dI/dt is used for spike detection, in the simplest scenario, T_{bkg1} is

at the interception of dl/dt with zero to the left of $T(dl/dt)_{max}$ (**Supplementary Fig. 1a**, point 2) and T_{bkg2} is the time-point at the same as T_{bkg1} current level to the right of T_{max} . The variability of possible spikes shapes and arrangements and the presence of noise however make it rather difficult to define spike baseline in all cases in a completely user-independent fashion. While additional algorithms presented below help to account for some possible complications during analysis, it is always advisable to visually examine the spikes and readjust their baselines if necessary.

The first algorithm improves baseline positioning on spikes with low signal/noise or those having slow-rising PSF, when $dl/dt=0$ fails to represent the true T_{bkg1} (**Supplementary Fig. 1c**). The program searches for a steady state that persists for certain duration ΔT_{min} , by first dividing the trace into ΔT_{min} segments and then comparing the average current values between the adjacent segments. Searching from T_{max} or $T(dl/dt)_{max}$ and reiteratively moving to the left, the steady state is found if two segments have the currents within one SD_I of each other. Next, T_{bkg1} is set to the first time-point at the steady state current. Spike width at $T(dl/dt)_{max}$ can be used as the initial ΔT_{min} value and it is essential to repeat the procedure with $2^* \Delta T_{min}$ or longer increments to account for the presence of PSF with a steady state. If longer increments result in lower steady state values, the latter should be used for T_{bkg1} calculation (**Supplementary Fig. 1d**). Obviously, some PSF with extremely long steady states may still be missed by this routine and their baseline should be readjusted manually. Additionally, it should be noted that this method employs SD_I to find the steady state and therefore is dependent on the degree of filtering applied to the trace.

When determining T_{bkg2} , an increasing contribution of high-frequency noise complicates the assessment of the time-point when the transmitter concentration reaches background

levels (**Supplementary Fig. 1e**). For the smallest spikes, this may underestimate the amperometric charge by 10-20% and introduce as much as a two-fold error in the exponential decay constants of the falling phase fits. To counter this, the search for T_{bkg2} can be performed on the trace additionally filtered with F_{c2} binomial filter (see above), which does not affect low frequencies present in the decaying phase of the spike but substantially decreases the artifacts associated with the presence of white noise.

Another difficulty that may interfere with proper baseline positioning is the presence of background drifts, such as in overlapping spikes; even if the overlaps will be discarded during the analysis, first they need to be recognized as such (see *Analysis of overlapping spikes* in the main text). While spikes with uneven baseline may not be preceded by steady states and the current at their baseline may not be at the I_{bkg} level, the beginning of these events can be found at $dl/dt=0$ (**Supplementary Fig. 1f**, spike 2). Similarly, the presence of background drifts may complicate the search for T_{bkg2} since it might not be at the same current level as T_{bkg1} or within one SD_1 of this value (**Supplementary Fig. 1f**, spike 1). A simple solution that works in this case is to set T_{bkg2} to the minimum of current that follows the spike. This minimum is found between the spike's T_{max} and the next spike maximum (if found) or the end of the trace. Although the above protocols for finding the baselines of the overlapping spikes are not very accurate on traces with high noise levels, their purpose is only to locate such events. Subsequently, the overlaps are either discarded or analyzed by separating them (**Supplementary Fig. 3** online). In the latter case, the beginning and the end of the overlap-containing event are refined using the same algorithms as for a singlet spike: T_{bkg1} is at the steady state current to the left of the first spike, and T_{bkg2} is at the same as T_{bkg1} current to the right of the last spike.

Primary cell cultures

Chemicals were purchased from Sigma (Milwaukee, WI). Rat chromaffin cells were prepared and cultured as previously described⁸. Cells were maintained in a 5% CO₂ incubator at 37°C. All measurements were conducted between days 3-4 post-plating. Animal protocols were approved by the Columbia University Institutional Animal Care and Use Committees.

Amperometric recordings

Solutions used for amperometric recordings were as follows. The bath saline contained (in mM): 128 NaCl, 2 KCl, 1 NaH₂PO₄, 2 MgCl₂, 1.2 CaCl₂, 10 glucose, 10 HEPES (pH 7.4). Stimulation solution was the same except for 90 NaCl and 40 KCl. A 5 μm diameter carbon fiber electrode held at +700 mV was positioned over a cell (Newport micromanipulator MX300R, Irvine, CA) and lowered until the latter was slightly depressed. No events were recorded when the applied voltage was adjusted to 0 mV or when the electrode was transiently lifted from the cell. The current was filtered using a 4-pole 5 kHz Bessel filter built into an Axopatch 200B amplifier (Axon Instruments, Foster City, CA) and sampled at 25 kHz (ITC-18, Instrutech, Great Neck, NY). Secretagogue was applied by local perfusion through a pressurized glass micropipette (Picospritzer, General Valve Corp., Fairfield, NJ) for 5 sec at ~10 μm from the cell. After secretagogues application, the amperometric current was recorded for 60 sec using a locally written routine in Igor Pro (Wave Metrics, Lake Oswego, OR). Data files were saved in Igor binary format for further analysis.

For catecholamine release, it is convenient to present the quantal size as the number of released molecules, N , which is related to electric charge, Q , as $N = Q / (n \times F)$, where F is Faraday's constant and n is the number of electrons donated by each catechol moiety^{9,10}:

$$N = Q [\text{pC}] \times 10^{-12} \left[\frac{\text{C}}{\text{pC}} \right] \times \frac{6.023 \times 10^{23} \left[\frac{\text{electrons}}{\text{mole}} \right]}{2 \left[\frac{\text{electrons}}{\text{molecule}} \right] \times 96,485 \left[\frac{\text{C}}{\text{mole}} \right]} = Q [\text{pC}] \times 3.121 \times 10^6 \left[\frac{\text{molecule}}{\text{pC}} \right]$$

Statistical analysis

Datasets in the tables were compared by Mann-Whitney rank sum test. The goodness of Gaussian fits was analysed by Wald-Wolfowitz (runs) test in Prism 4 (GraphPad Software Inc.).

1. Heinemann, S.H. in *Single-Channel Recording* (eds. Sakmann, B. & Neher, E.) 53-91 (Plenum Press, New York, 1995).
2. Colquhoun, D. & Sigworth, F.J. in *Single-Channel Recording* (eds. Sakmann, B. & Neher, E.) 483-587 (Plenum Press, New York, 1995).
3. Marchand, P. & Marmet, L. Binomial smoothing filter: A way to avoid some pitfalls of least-squares polynomial smoothing. *Rev. Sci. Instrum.* **54**, 1034-1041 (1983).
4. Gomez, J.F. *et al.* New approaches for analysis of amperometrical recordings. *Ann. NY Acad. Sci.* **971**, 647-654 (2002).
5. Segura, F. *et al.* Automatic analysis for amperometrical recordings of exocytosis. *J. Neurosci. Methods* **103**, 151-156 (2000).
6. Schroeder, T.J. *et al.* Temporally resolved, independent stages of individual exocytotic secretion events. *Biophys. J.* **70**, 1061-1068 (1996).
7. Chow, R.H. & von Ruden, L. in *Single-channel recording* (eds. Sakmann, B. & Neher, E.) 245-276 (Plenum Press, New York, 1995).
8. Mosharov, E. *et al.* Intracellular Patch Electrochemistry: Regulation of Cytosolic Catecholamines in Chromaffin Cells. *J. Neurosci.* **23**, 5835-5845 (2003).
9. Kissinger, P.T., Hart, J.B. & Adams, R.N. Voltammetry in brain tissue-a new neurophysiological measurement. *Brain Res.* **55**, 209-213 (1973).

10. Baur, J.E. *et al.* Fast-scan voltammetry of biogenic amines. *Anal. Chem.* **60**, 1268-1272 (1988).